

# Accepted Manuscript

Structural and Mechanical properties of transition metal borides  $Nb_2MB_2$  ( $M = Tc, Ru,$   
and Os) under pressure

Xiaofeng Li, Haiyan Yan, Qun Wei



PII: S2352-2143(15)30024-1

DOI: [10.1016/j.cocom.2016.02.001](https://doi.org/10.1016/j.cocom.2016.02.001)

Reference: COCOM 36

To appear in: *Computational Condensed Matter*

Received Date: 30 November 2015

Revised Date: 14 February 2016

Accepted Date: 14 February 2016

Please cite this article as: X. Li, H. Yan, Q. Wei, Structural and Mechanical properties of transition metal borides  $Nb_2MB_2$  ( $M = Tc, Ru,$  and Os) under pressure, *Computational Condensed Matter* (2016), doi: 10.1016/j.cocom.2016.02.001.

This is a PDF file of an unedited manuscript that has been accepted for publication. As a service to our customers we are providing this early version of the manuscript. The manuscript will undergo copyediting, typesetting, and review of the resulting proof before it is published in its final form. Please note that during the production process errors may be discovered which could affect the content, and all legal disclaimers that apply to the journal pertain.

# Structural and Mechanical properties of transition metal borides Nb<sub>2</sub>MB<sub>2</sub> (M = Tc, Ru, and Os) under pressure

Xiaofeng Li<sup>a,\*</sup>, Haiyan Yan<sup>b</sup>, Qun Wei<sup>c</sup>

<sup>a</sup> College of Physics and Electronic Information, Luoyang Normal College, Henan Luoyang, 471022, PR China

<sup>b</sup> College of Chemistry and Chemical Engineering, Baoji University of Arts and Sciences, Baoji 721013, PR China

<sup>c</sup> School of Physics and Optoelectronic Engineering, Xidian University, Xi'an 710071, PR China

## ABSTRACT

First-principle total energy calculations are employed to provide a fundamental understanding of the structural, mechanical, and electronic properties of transition metal borides Nb<sub>2</sub>MB<sub>2</sub> (M = Tc, Ru, and Os) within the tetragonal superstructure *P4/mnc* structure. The mechanically and dynamically stabilities of three borides have been demonstrated by the elastic constants and phonons calculations under pressure. Among these three compounds, Nb<sub>2</sub>TcB<sub>2</sub> exhibits the biggest bulk and Young's modulus, smallest Poisson's ratio, and highest harness. Density of states of them revealed that the strong B-B, Nb-B and M-B covalent bonds are major driving forces for their high bulk and shear moduli as well as small Poisson's ratio.

*Keywords:* First-principles calculations; Transition metal borides; Mechanical properties

---

\* Corresponding author. Tel. / fax: +86 379 65515016. E-mail address: [lxfdjy@126.com](mailto:lxfdjy@126.com)

## 1. Introduction

A central challenge to modern material science is the rational design and synthesis of new material possessing appealing properties. Among these, looking for novel hard or superhard materials is one of the very important subjects. Ultra-incompressible hard materials are widely used in various industrial applications, such as cutting tools, high-temperature environments, and hard coating [1-3]. In recent years, great efforts have been devoted to search for new superhard materials. One approach is to synthesize light element compounds consisted of boron, carbon, nitrogen, and oxygen, for instance, diamond, cubic boron nitride (*c*-BN), and carbon nitrides, etc [4-6]. However, at high temperature, diamond is not only unstable in the presence of oxygen, but also reacts easily with iron-containing materials; another new design principle was proposed to synthesize ultra-hard materials by combining small, strong covalent bonding atoms such as B, C or N with large, electron-rich transition metals, for example ReB<sub>2</sub> [7-9]. The introduction of light elements improves the hardness of the transition metal by forming a strong covalent interaction between the TM and the light elements, and between the light elements. Especially transition metal (M) borides, as a type of potential very hard or superhard material [10], have been recently received noticeable attention. In the past years, many scientists concentrated on studying the relationship between hardness and bond states, structure and composition of these TMBs [11-15]. The electronic and elastic properties of many transition metal borides at ambient condition have been investigated, and the obtained results have pointed out that binary transition metal borides possess excellent mechanical properties [16].

Nowadays, some transition metal borides with U<sub>3</sub>Si<sub>2</sub>-type structure have been applied in cermets applications and these borides showed promising mechanical properties like ultra-incompressibility and corrosion resistance [17-19]. Recently, a new synthesized transition metal boride Nb<sub>2</sub>OsB<sub>2</sub> [20] crystallized a twofold superstructure (space group *P4/mnc*, No.128) of the tetragonal U<sub>3</sub>Si<sub>2</sub>-type, which is different from the Zr<sub>3</sub>Al<sub>2</sub> superstructure [21]. This superstructure can be described as the intergrowth of CsCl and AlB<sub>2</sub> structure types. So far, there are a few studies on mechanical and electronic properties of A<sub>2</sub>MB<sub>2</sub> (A, M represented transition metal) experimentally and theoretically. The first principle was adopted to investigate the mechanical properties and electronic structure for Mo<sub>2</sub>FeB<sub>2</sub> [22]. Fokwa *et. al.* [23] investigated theoretically the electronic structure and magnetism of Nb<sub>2</sub>MB<sub>2</sub> (M=Fe, Ru, Os) in Mo<sub>2</sub>FeB<sub>2</sub> and Nb<sub>2</sub>OsB<sub>2</sub>

structure types. Subsequently, the influences of chemical bonding and electronic structure on the elastic properties in the  $A_2MB_2$  series ( $A = Nb, Ta; M = Fe, Ru, Os$ ) were studied by Fokwa *et. al.* [24], and it was found that the bulk and shear modulus are both affected by the strength of the chemical bonding and the position of the Fermi level in the density-of-states. More recently, the elastic properties, hardness and electronic structure of  $Nb_2MB_2$  ( $M=Mo, W, Re$  and  $Os$ ) are investigated at ambient condition [25]. It revealed that the covalence between Nb-4*d* as well as M-*nd* ( $n=4$  for Mo and 5 for W, Re and Os) and B-2*p* states, are the cause of the relatively higher elastic modulus and hardness of Nb-based compounds. In order to search new ultra-compressible materials, we proposed the ternary niobium borides  $Nb_2MB_2$  ( $M = Ru, Tc$ ), which have not been synthesized. So far, the mechanical and lattice thermodynamic properties of  $Nb_2MB_2$  ( $M=Os, Ru, Tc$ ) under pressure are still puzzling. Moreover, thermodynamic consideration of stability for a crystal is very important in searching for hard materials. Therefore, in this work, the structural stability, elastic properties, electronic, and thermodynamic properties of the systems  $Nb_2MB_2$  ( $M=Os, Ru, Tc$ ) under pressure are systematically investigated. The purpose of this work is to provide some helpful guidance for the future search of novel superhard materials.

## 2. Computational Methods

The *ab initio* structural relaxations and electronic structure calculations were performed using density functional theory with the Perdew-Burke-Ernzerhof (PBE) generalized gradient approximation (GGA) of the exchange-correlation energy as implemented in the VASP code [26]. The projector augmented wave (PAW) method was employed to model the electron-ion interaction in the valence space. A cutoff energy of 600 eV was used for the plane wave expansion of the wave functions, and fine regular *k*-point grids  $10 \times 10 \times 8$  (used for Brillouin zone integrations) [27], to ensure that all the enthalpy calculations were converged to better than 1 meV/atom. Single crystal elastic constants were determined from evaluation of stress tensor generated small strain and bulk modulus, shear modulus, Young's modulus, and Poisson's ratio were thus estimated by using the Voigt-Reuss-Hill approximation [28]. Phonon calculations were carried out using a supercell approach as implemented in the PHONOPY code [29].

## 3. Results and discussion

All  $Nb_2MB_2$  ( $M = Tc, Ru, Os$ ) phases crystallize in a twofold superstructure, which is

showed in Fig. 1. It can be seen that this  $P4/mnc$  phase consists of a fundamental chain along the  $c$ -axis. In this chain, all the M atoms are eightfold coordinated with eight Nb and each M atom is located at the center of it. The lattice structure and ionic positions are all fully optimized, and the equilibrium lattice constants  $a$ ,  $c$ ,  $c/a$ , and bond length are listed in Table 1, together with the available experimental data [21] and theoretical results[24-26]. In order to compare the phase stability of  $Nb_2MB_2$ , the relations of the energy and volume of three borides are calculated and the results are showed in Fig. 2. We can easily found that the phase stability sequence is:  $Nb_2OsB_2 > Nb_2TcB_2 > Nb_2RuB_2$ . The bulk modulus is obtained by fitting pressures and cell volumes with the third-order Birch-Murnaghan equation of state (EOS) [30]. The calculated bulk modulus is 284 GPa, 280 GPa and 354 GPa for  $Nb_2TcB_2$ ,  $Nb_2RuB_2$  and  $Nb_2OsB_2$ , respectively, which indicated that they are all the incompressible materials (the incompressible sequence is  $Nb_2OsB_2 > Nb_2TcB_2 > Nb_2RuB_2$ ). From Table 1, we can find that all these theoretical data can be competitive with the experimental and theoretical ones. However, the compounds  $Nb_2RuB_2$  and  $Nb_2TcB_2$  have not been synthesized, and there are no available experimental data for comparison. Therefore, the present results could provide useful information for further experimental or theoretical investigations.

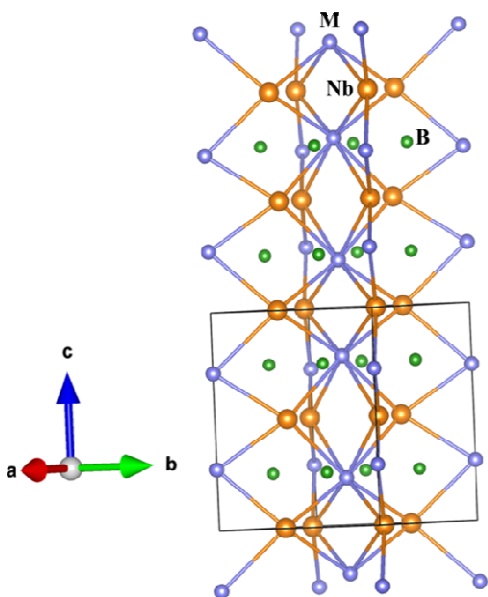


Fig.1 The crystal structure of  $Nb_2MB_2$   
( $M=Tc, Ru$  and  $Os$ )

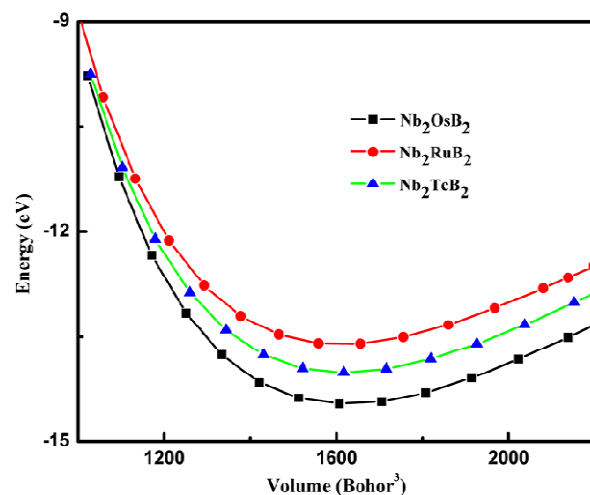


Fig.2 The relations of Energy and Volume of  
 $Nb_2MB_2$  ( $M=Tc, Ru$  and  $Os$ )

Table 1 The lattice parameters  $a$  (Å),  $c$  (Å),  $c/a$ , bulk modulus  $B_0$  (GPa), the formation enthalpy  $\Delta H$  (eV) and the bond length ofNb<sub>2</sub>MB<sub>2</sub> (M= Tc, Ru and Os)

	$a$	$c$	$c/a$	$B_0$	$\Delta H$	B-B	Nb-M	Nb-B	M-B
Nb <sub>2</sub> TcB <sub>2</sub>	6.026	6.601	1.095	284	-3.433	1.886	2.766	2.424	2.439
Nb <sub>2</sub> RuB <sub>2</sub>	5.661	6.483	1.152	280	-3.196	1.873	2.717	2.412	2.397
Nb <sub>2</sub> OsB <sub>2</sub>	5.901	6.868	1.116	354	-4.185	1.889	2.722	2.408	2.386
	5.922 <sup>[20]</sup>	6.879 <sup>[20]</sup>	1.162						
	5.939 <sup>[23]</sup>	6.891 <sup>[23]</sup>							
	5.926 <sup>[25]</sup>	6.894 <sup>[25]</sup>	1.163 <sup>[25]</sup>	297 <sup>[25]</sup>					

All Nb<sub>2</sub>MB<sub>2</sub> (M = Tc, Ru, Os) phases crystallize in a twofold superstructure, which is showed in Fig. 1. It can be seen that this  $P4/mnc$  phase consists of a fundamental chain along the  $c$ -axis. In this chain, all the M atoms are eightfold coordinated with eight Nb and each M atom is located at the center of it. The lattice structure and ionic positions are all fully optimized, and the equilibrium lattice constants  $a$ ,  $c$ ,  $c/a$ , and bond length are listed in Table 1, together with the available experimental data [20] and theoretical results[23-25]. In order to compare the phase stability of Nb<sub>2</sub>MB<sub>2</sub>, the relations of the energy and volume of three borides are calculated and the results are showed in Fig. 2. We can easily found that the phase stability sequence is: Nb<sub>2</sub>OsB<sub>2</sub> > Nb<sub>2</sub>TcB<sub>2</sub> > Nb<sub>2</sub>RuB<sub>2</sub>. The bulk modulus is obtained by fitting pressures and cell volumes with the third-order Birch-Murnaghan equation of state (EOS) [30]. The calculated bulk modulus is 284 GPa, 280 GPa and 354 GPa for Nb<sub>2</sub>TcB<sub>2</sub>, Nb<sub>2</sub>RuB<sub>2</sub> and Nb<sub>2</sub>OsB<sub>2</sub>, respectively, which indicated that they are all the incompressible materials (the incompressible sequence is Nb<sub>2</sub>OsB<sub>2</sub> > Nb<sub>2</sub>TcB<sub>2</sub> > Nb<sub>2</sub>RuB<sub>2</sub>). From Table 1, we can find that all these theoretical data can be competitive with the experimental and theoretical ones. However, the compounds Nb<sub>2</sub>RuB<sub>2</sub> and Nb<sub>2</sub>TcB<sub>2</sub> have not been synthesized, and there are no available experimental data for comparison. Therefore, the present results could provide useful information for further experimental or theoretical investigations.

Meanwhile, it is important to explore the thermodynamic stability of Nb<sub>2</sub>MB<sub>2</sub> for further experimental synthesis. The thermodynamic stability at ambient condition with respect to decomposition is quantified in terms of the formation enthalpy, which is calculated by the

following formula:

$$H_f = H(\text{Nb}_2\text{OsB}_2) - 2H(\text{Nb}) - H(\text{M}) - 2H(\text{B}) \quad (1)$$

in which the  $H_f$  is the formation enthalpy, the body-centered-cubic Tc and Ru (space group:  $Im-3m$ ), hexagonal Os and Nb (space group:  $P6_3/mmc$ ), and  $\alpha$ -B (space group:  $R-3m$ ) were chosen as the reference phases. As shown in Table 1, the calculated formation enthalpies of these borides per atom are -0.6392 eV, -0.6866 eV and -0.837 eV for  $\text{Nb}_2\text{RuB}_2$ ,  $\text{Nb}_2\text{TcB}_2$  and  $\text{Nb}_2\text{OsB}_2$ , respectively. It indicated that the thermodynamic stability is in proper order:  $\text{Nb}_2\text{OsB}_2 > \text{Nb}_2\text{TcB}_2 > \text{Nb}_2\text{RuB}_2$ , which is in consistent with the results from Fig. 2.

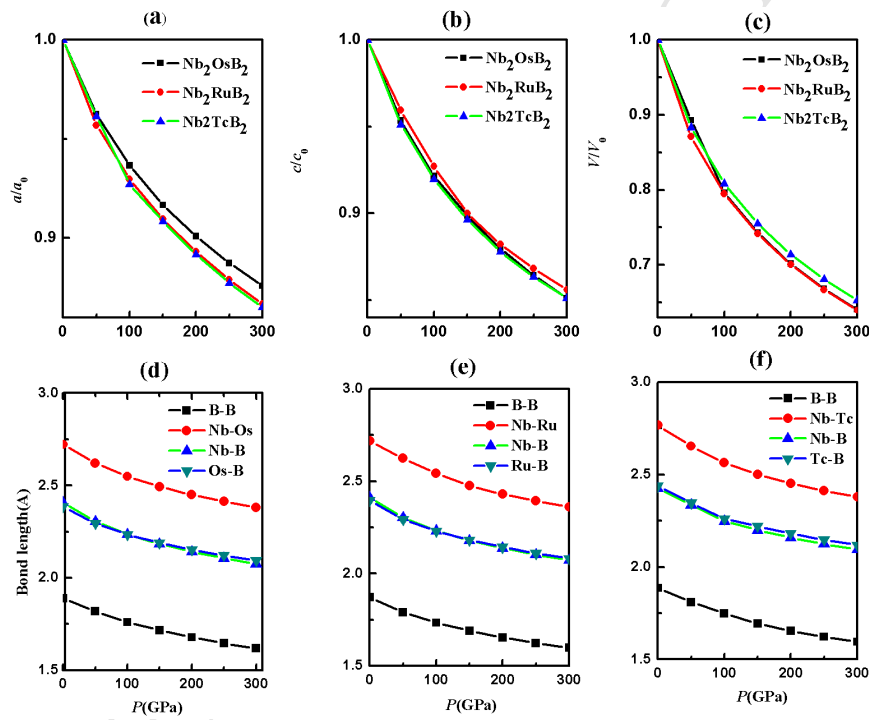


Fig.3 The normalized (a)  $a/a_0$  (b)  $c/c_0$  (c)  $V/V_0$  of  $\text{Nb}_2\text{MB}_2$  ( $M=\text{Tc, Ru and Os}$ ); (d) the pressure dependence on the bond length of (d)  $\text{Nb}_2\text{OsB}_2$  (e)  $\text{Nb}_2\text{RuB}_2$  (f)  $\text{Nb}_2\text{TcB}_2$ .

In order to provide some insights into the pressure behavior of  $\text{Nb}_2\text{OsB}_2$ , the changes of lattice constants and cell volume with pressure are plotted in Fig. 3. For simplicity, the ratios  $a/a_0$ ,  $c/c_0$  and  $V/V_0$  are shown in Fig. 3, where  $a_0$ ,  $c_0$  and  $V_0$  are the zero pressure equilibrium structural parameters and volume. From Fig. 3, firstly, it can be seen that the in-compressibility along the  $a$ -axis is stronger than that along the  $c$  axis for  $\text{Nb}_2\text{MB}_2$  compounds, suggesting their clear elastic anisotropy. Moreover, along  $a$  axis, the incompressibility is almost identical for  $\text{Nb}_2\text{RuB}_2$  and  $\text{Nb}_2\text{TcB}_2$ , and  $\text{Nb}_2\text{OsB}_2$  is the most incompressible. Along  $c$  axis, incompressibility of  $\text{Nb}_2\text{MB}_2$  is almost equal and the  $\text{Nb}_2\text{RuB}_2$  is slightly stronger. The volume incompressibility is

similar to that of  $c/c_0$ . However,  $\text{Nb}_2\text{TcB}_2$  in volume compressibility is a little stronger. The relations between bond length and pressure are also exhibited in Fig. 3. The curve of bond lengths with pressure is almost parallel for B-B, Nb-Os, Nb-B and Os-B. Moreover, the variations of bond lengths are smaller with pressure (about 12% from 0 GPa to 300 GPa), and the bond length of Nb-Os reduced littlest, which indicated that the  $\text{Nb}_2\text{MB}_2$  compounds have strong incompressibility under pressure. Dynamic stability is important for structural stability and can be evaluated from the phonon spectra. The phonon dispersion curves in the whole Brillouin zone (BZ) of the  $\text{Nb}_2\text{MB}_2$  compounds under pressures (0 GPa and 300 GPa) are shown in Fig. 4. There is no imaginary frequency in the whole BZ, which indicates dynamic stability of these compounds under pressures.

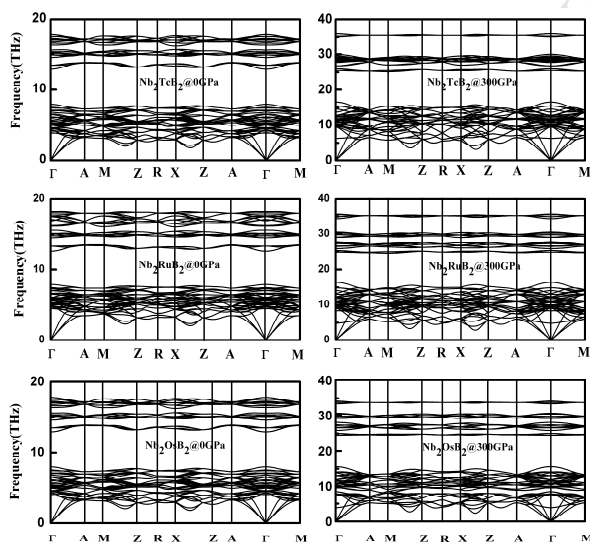


Fig.4 The phonon dispersion curves of  $\text{Nb}_2\text{MB}_2$  (M=Tc, Ru and Os) under 0GPa and 300GPa.

The mechanical properties (elastic constants and elastic moduli) are essential for understanding the macroscopic mechanical properties of solids and for the design of hard materials and their potential technological applications. Accurate elastic constants can directly describe the response of a crystal to external stresses (i.e., its initial deformation and recovery to its original shape after the stress ceases). The zero pressure elastic constants  $C_{ij}$  and other relevant modulus of  $\text{Nb}_2\text{MB}_2$  (M =Tc, Ru and Os) were calculated by the strain-stress method, which are listed in Table 2, together with the available theoretical data [24, 25]. For the tetragonal crystal to be mechanically stable, its elastic constants should obey the following inequalities [31]:



$$C_{11} > |C_{12}|, 2C_{13}^2 < C_{33}(C_{11} + C_{12}), C_{44} > 0, C_{66} > 0 \quad (2)$$

Obviously, all Nb<sub>2</sub>MB<sub>2</sub> compounds are mechanically stable under ambient conditions. It also can be seen that these compounds have larger  $C_{11}$  than  $C_{33}$ , which manifested that their a-axis is more in-compressible than that along  $c$ -axis directions. Elastic constant  $C_{44}$  is an important parameter of the material's indentation hardness. The  $C_{44}$  value of Nb<sub>2</sub>TcB<sub>2</sub> (203 GPa) is the largest one, which indicated that Nb<sub>2</sub>TcB<sub>2</sub> has the strong resistance to shear stress. Based on the calculated elastic constants, the bulk modulus  $B$  and shear modulus  $G$  of polycrystalline are calculated by the Voigt-Reuss-Hill approximation in Table 2. It reveals that Nb<sub>2</sub>OsB<sub>2</sub> has the largest bulk and shear modulus, which means that it possess the highest incompressibility. The Young's modulus  $E$  and Poisson's ratio  $\nu$  are important for technological and engineering applications. Young's modulus  $E$  and Poisson's ratio  $\nu$  are used to provide a measure of the stiffness and properties about bonding forces of the solid. They can be obtained from the following equations:

$$E = 9BG/(3B + G), \nu = (3B - 2G)/2(3B + G) \quad (3)$$

The calculated values are also showed in Table 2. Nb<sub>2</sub>TcB<sub>2</sub> is found to have the highest Young's modulus (452 GPa) and lowest Poisson's ratio (0.226). They are two important elastic tensors, which are identified to be strongly correlated to hardness.

Table 2 The calculated elastic constants  $C_{ij}$  (GPa), the bulk modulus  $B$  (GPa), shear modulus  $G$  (GPa), Young modulus  $E$  (GPa),  $B/G$ , Poisson ratio  $\nu$  and the hardness  $Hv$  (GPa) of Nb<sub>2</sub>MB<sub>2</sub> (M= Tc, Ru and Os).

	$C_{11}$	$C_{33}$	$C_{44}$	$C_{66}$	$C_{12}$	$C_{13}$	$B$	$G$	$E$	$B/G$	$\nu$	$Hv$
Nb <sub>2</sub> TcB <sub>2</sub>	538	452	203	176	120	180	276	184	452	1.496	0.226	23.4
Nb <sub>2</sub> RuB <sub>2</sub>	506	409	184	172	130	194	270	165	412	1.655	0.248	19.2
Ref[25]							272	146	371	1.86	0.27	
Nb <sub>2</sub> OsB <sub>2</sub>	555	420	199	185	142	224	300	189	437	1.727	0.257	20.2
Ref [25]	576	477	216	187	137	195	298	195	480	1.528	0.231	24.1
Ref [24]							289	153	390	1.89	0.28	

The obtained elastic constants, bulk modulus  $B$ , shear modulus  $G$  and Young modulus  $E$  at different pressures are presented in Fig. 5. It is found that all the elastic constants increase with different rate with increasing pressure. The dependences of elastic constants on pressure of  $C_{11}$ ,  $C_{22}$ ,  $C_{33}$ ,  $C_{44}$ ,  $C_{12}$ ,  $C_{13}$ ,  $B$ ,  $G$  and  $E$  for the  $\text{Nb}_2\text{OsB}_2$  are 5.261 (5.508, 5.816), 4.268 (4.618, 4.904), 1.854 (1.856, 2.006), 1.314 (1.376, 1.496), 2.508 (2.690, 2.606), 3.234 (3.490, 3.328), 3.646 (3.868, 3.972), 1.296 (1.342, 1.536), 3.564 (3.704, 4.186), respectively. Therefore, the values of  $C_{11}$ ,  $C_{22}$ ,  $C_{33}$ ,  $C_{13}$ , bulk modulus  $B$ , shear modulus  $G$  and Young modulus  $E$  of these three compounds increase faster than other elastic modulus. Moreover, the relevant elastic tensors of  $\text{Nb}_2\text{TcB}_2$  increases quickest except  $C_{12}$  and  $C_{13}$  ( $C_{12}$  and  $C_{13}$  vary fastest for  $\text{Nb}_2\text{RuB}_2$ ). Poisson's ratio (Fig.6 (a)) increases in response to pressure;  $\text{Nb}_2\text{TcB}_2$  has the smallest Poisson's ratio, and above about 73 GPa the Poisson's ratio has higher value for  $\text{Nb}_2\text{RuB}_2$  than that of  $\text{Nb}_2\text{OsB}_2$ . These results indicated  $\text{Nb}_2\text{TcB}_2$  possibly corresponds to the highest hardness in three compounds.

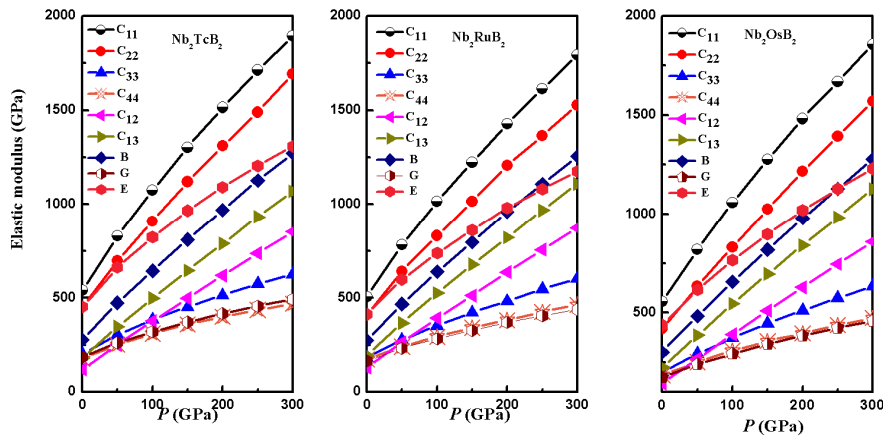


Fig.5 The relevant elastic tensors of  $\text{Nb}_2\text{MB}_2$  ( $M=\text{Tc}$ ,  $\text{Ru}$  and  $\text{Os}$ ) under pressure

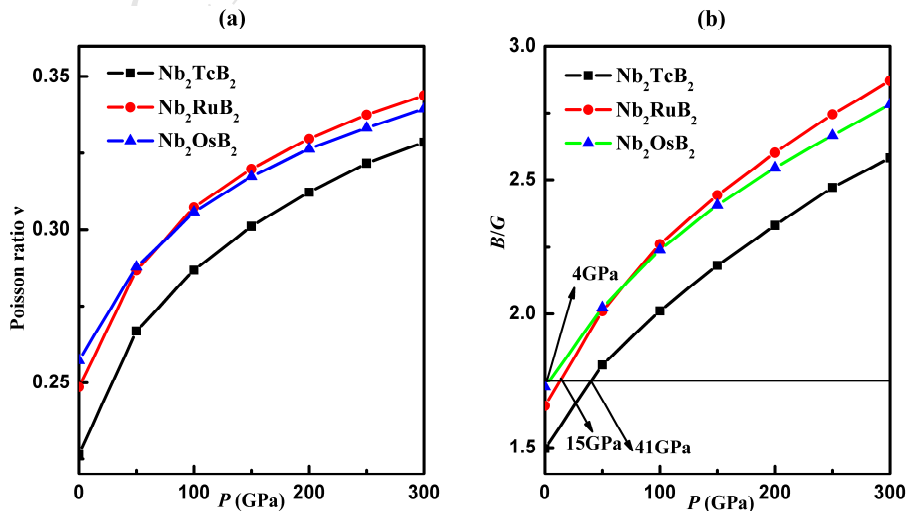


Fig. 6 Poisson ratio (a) and  $B/G$  (b) under pressure of  $\text{Nb}_2\text{MB}_2$  ( $M=\text{Tc}$ ,  $\text{Ru}$  and  $\text{Os}$ ).

To evaluate the brittleness of materials, Pugh [32] introduced the  $B/G$  ratio. The critical value of  $B/G$  ratio, 1.75, is regarded as boundary to divide the material is brittleness or ductility [33]. If the ratio is less than 1.75, the material is considered to be brittle, otherwise, the material is considered to be ductile. For the  $Nb_2MB_2$  compounds, the  $B/G$  ratios are both smaller than 1.75, so these materials are brittle. Among them, the sequence of brittleness of  $Nb_2MB_2$  is  $Nb_2TcB_2 > Nb_2RuB_2 > Nb_2OsB_2$ .  $Nb_2TcB_2$  has the biggest brittleness. Under pressure (Fig. 6(b)), the values of  $B/G$  increases for three compounds. When pressures arrived to about 41 GPa, 15 GPa, and 4 GPa for  $Nb_2TcB_2$ ,  $Nb_2RuB_2$  and  $Nb_2OsB_2$ , respectively, they transformed from brittleness to ductility. Above 73 GPa,  $Nb_2RuB_2$  has strongest ductility.

The hardness of a material always plays an important role in its applications, especially for in-compressional phase. Vickers hardness  $H_v$  is not only associated with the shear modulus  $G$ , but also the bulk modulus  $B$  for many materials. The hardness can be obtained from the following correlations by Chen et al. [34]:

$$H_v = 2(k^2G)^{0.585} - 3 \quad (4)$$

Nevertheless, Tian *et al.* [35] reported that there is a little error in the equation presented by Chen et.al due to the “-3” term, so they modified it which then can always obtain accurate values. Therefore, in present work, we use the amendatory equation by Tian et.al.:

$$H_v = 0.92k^{1.137}G^{0.708}, k = G/B \quad (5)$$

The calculated Vicker hardness of three  $Nb_2MB_2$  compounds by Eq. (5) and are listed in Table 2. We can find that  $Nb_2TcB_2$  has the highest hardness (23.4 GPa) and the hardness of  $Nb_2RuB_2$  and  $Nb_2TcB_2$  are 19.4 GPa and 20.2 GPa, respectively, which are close to each other.

Based on the fundamental elastic constants, a useful visualization of the elastic anisotropy can be obtained by plotting three-dimensional picture of dependence of the Young's modulus  $E$  on a direction in crystal. For tetragonal solid, by the following equation the Young's modulus  $E$  can be expressed as [36]:

$$E^{-1} = s_{11}(\alpha^4 + \beta^4) + s_{33}\gamma^4 + 2s_{12}\alpha^2\beta^2 + 2s_{13}(\beta^2\gamma^2 + \alpha^2\gamma^2) + s_{44}(\beta^2\gamma^2 + \alpha^2\gamma^2) + s_{66}\alpha^2\beta^2 \quad (6)$$

where  $\alpha$ ,  $\beta$ , and  $\gamma$  are the direction cosines of  $[uvw]$  direction. The three-dimensional surface representations showing the variation of Young's modulus are plotted in Fig. 7. For crystals, the degree of elastic anisotropy can be directly reflected from the degree of deviation in shape from

a sphere. As shown in Fig.7, three  $\text{Nb}_2\text{MB}_2$  compounds exhibit the elastic anisotropies since the shape of the Young's modulus representation deviates from a spherical shape, in which they have similar shapes. Fig. 8 showed the variation of Young's modulus in the (001) plane for the quadrant of directions  $[uvw]$  between  $[100]$  ( $\theta=0^\circ$ ) and  $[010]$  ( $\theta=90^\circ$ ). It is clearly seen that Young's moduli of three  $\text{Nb}_2\text{MB}_2$  compounds exhibit little changes on the whole orientation, and  $\text{Nb}_2\text{RuB}_2$  and  $\text{Nb}_2\text{OsB}_2$  possesses a nearly equal minimum of  $E_{[100]} = E_{[010]} = 389$  GPa and a maximum of  $E_{[011]} = 493$  GPa. For the (100) plane in Fig. 8, it can be found that the variation of Young's modulus for directions  $[0vw]$  between  $[001]$  ( $\theta=0^\circ$ ) and  $[010]$  ( $\theta=90^\circ$ ), the variation tendencies of Young's moduli for three compounds are all similar with  $E_{[001]} = 355/290/292$  GPa and  $E_{[011]} = 493/453/455$  GPa for  $\text{Nb}_2\text{TcB}_2/\text{Nb}_2\text{RuB}_2/\text{Nb}_2\text{OsB}_2$ . The Young's modulus of three  $\text{Nb}_2\text{MB}_2$  compounds decrease quickly from  $[001]$  to  $[110]$  directions within the  $(1\bar{1}0)$  plane.

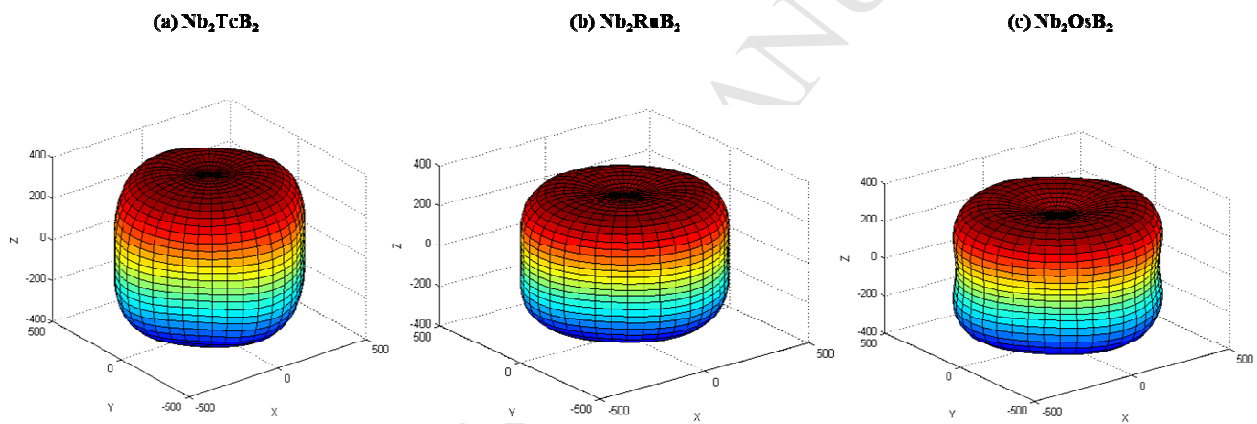


Fig.7 Three-dimensional surface representations of Young's modulus for (a)  $\text{Nb}_2\text{TcB}_2$ , (b)  $\text{Nb}_2\text{RuB}_2$ , (c)  $\text{Nb}_2\text{OsB}_2$ .

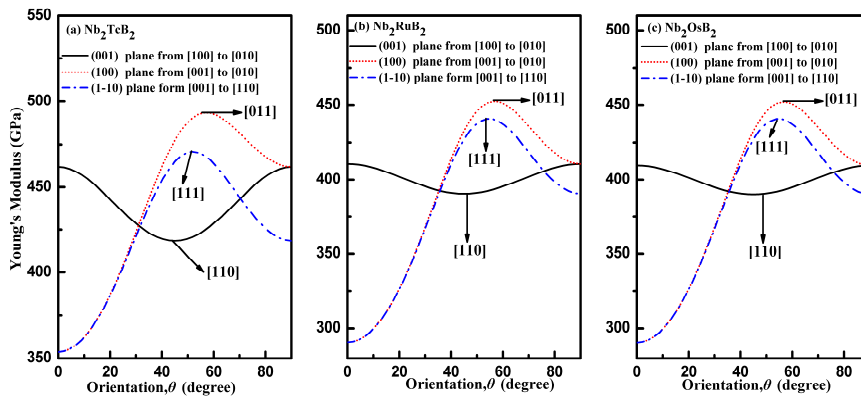


Fig.8 Orientation dependence of the Young's modulus for (a)  $\text{Nb}_2\text{TcB}_2$ , (b)  $\text{Nb}_2\text{RuB}_2$ , and (c)  $\text{Nb}_2\text{OsB}_2$ .

To understand plastic deformations in  $\text{Nb}_2\text{MB}_2$ , the variations of the shear modulus on

stress direction is also plotted in Fig. 9. The shear modulus  $G$  on the  $(hkl)$  shear plane with shear stress applied along  $[uvw]$  direction is given by:

$$G^{-1} = 4s_{11}(\alpha_1^2\alpha_2^2 + \beta_1^2\beta_2^2) + 4s_{33}\gamma_1^2\gamma_2^2 + 8s_{12}\alpha_1\alpha_2\beta_1\beta_2 + s_{66}(\alpha_1\beta_2 + \alpha_2\beta_1)^2 + 8s_{13}(\beta_1\beta_2\gamma_1\gamma_2 + \alpha_1\alpha_2\gamma_1\gamma_2) + s_{44}[(\beta_1\gamma_2 + \beta_2\gamma_1)^2 + (\alpha_1\gamma_2 + \alpha_2\gamma_1)^2] \quad (7)$$

where  $\alpha_1, \beta_1, \gamma_1, \alpha_2, \beta_2, \gamma_2$  are the direction cosines of the  $[uvw]$  and  $[HKL]$  directions in the coordinate systems, where the  $[HKL]$  denotes the vector normal to the  $(hkl)$  shear plane. In Fig.9, in all the shear planes, the variation tendencies of shear moduli of  $\text{Nb}_2\text{MB}_2$  compounds are similar. For shear plane (001) with the shear stress direction rotated from  $[100]$  to  $[010]$ , the direction cosines are  $\alpha_1 = \cos\theta, \beta_1 = \sin\theta, \gamma_1 = 0, \alpha_2 = \beta_2 = 0,$  and  $\gamma_2 = 1,$  where  $\theta$  is the angle between the  $[100]$  and shear stress direction. From Equation (7), we can obtain the shear modulus  $G = 1/s_{44} = C_{44},$  which means that the shear modulus of the  $\text{Nb}_2\text{MB}_2$  within (001) plane is independent of the shear stress direction. For shear plane (100) with the shear stress directions  $[0vw]$  varying from  $[100]$  to  $[010],$  the direction cosines are  $\alpha_1 = 0, \beta_1 = \sin\theta, \gamma_1 = \cos\theta, \alpha_2 = 1, \beta_2 = \gamma_2 = 0,$  and  $G^{-1} = s_{66} + (s_{44} - s_{66}) \cos^2 \theta,$  Because of  $s_{44} < s_{66}$  in three  $\text{Nb}_2\text{MB}_2$  compounds, their shear modulus are the smallest along  $[010]$  and the largest along  $[110].$

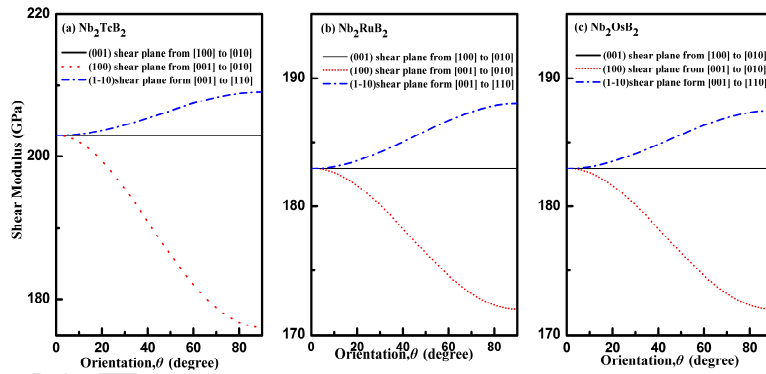


Fig.9 Orientation dependence of the shear modulus for (a)  $\text{Nb}_2\text{TcB}_2,$  (b)  $\text{Nb}_2\text{RuB}_2,$  and (c)  $\text{Nb}_2\text{OsB}_2.$

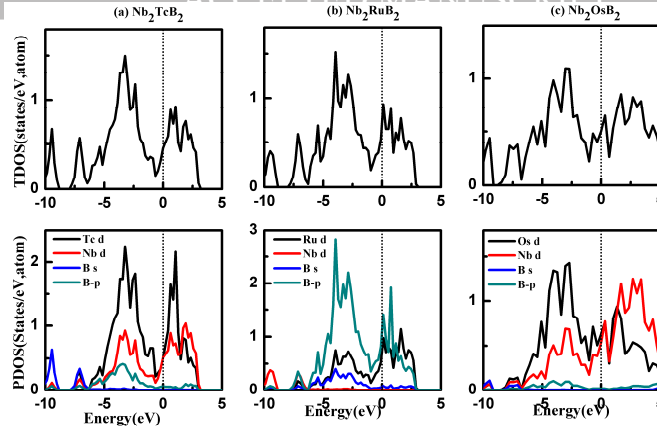


Fig. 10 The total and partial density of states of (a)  $\text{Nb}_2\text{TcB}_2$  (b)  $\text{Nb}_2\text{RuB}_2$  (c)  $\text{Nb}_2\text{OsB}_2$

In order to elucidate the origin of the mechanical properties of osmium borides, we show the calculated total (TDOS) and partial density of states (PDOS) in Fig. 10. There is no band gap in the DOSs at the Fermi level ( $E_F$ ), indicating the metallicity of these  $\text{Nb}_2\text{MB}_2$  compounds. An intriguing characterization of bonding is seen in the PDOS of  $\text{Nb}_2\text{MB}_2$  compounds, in which the Nb, M and boron atoms form strong covalent bonds, which are confirmed by the appreciable overlap of the Nb and M d-electron and the boron p-electron curves. In addition, the strong hybridization between B and B atoms forms the B–B covalent bonds. From Fig. 10, it can be found that the density of states of M d-state is larger than that of Nb d state under Fermi level, and above Fermi level the profiles of Nb-d and M-d electrons crossed except  $\text{Nb}_2\text{OsB}_2$ . Moreover, the deep valley near  $E_F$  is denoted the pseudogap, which separates the bonding and antibonding states. As shown from profile of total density of states in Fig.10, the deep valleys of these compounds near  $E_F$  indicated that the Nb (M) (d)–B(p) bonding states are saturated. The nearly full occupation of the bonding states and a vacant anti-bonding state leads to high elastic modulus, smaller Poisson's modulus and high hardness.

#### 4. Conclusions

In summary, we have performed systematic first-principles calculations to examine comprehensively the structural stability, mechanical properties, Vickers hardness and electronic structure of  $\text{Nb}_2\text{MB}_2$  ( $M=\text{Tc}$ ,  $\text{Nb}$ , and  $\text{Os}$ ) with  $P4/mnc$  superstructure under high pressure. The calculated equilibrium constants at ambient condition are in good agreement with the available theoretical and experimental data. The calculated elastic constants and phonon dispersions under pressure up to 300GPa indicated that these three  $\text{Nb}_2\text{MB}_2$  are mechanically and

thermodynamically stable. The calculated bulk modulus of three Nb<sub>2</sub>MB<sub>2</sub> compounds are all above 200GPa, which showed that they are all in-compressible material. Though energy-volume relation and formation enthalpies, Nb<sub>2</sub>OsB<sub>2</sub> is the most stable compound among three compounds, Nb<sub>2</sub>TcB<sub>2</sub> exhibits the biggest bulk and Young's modulus, smallest Poission's ratio and highest harness. The electronic properties of them indicated that the strong covalent Nb–B, M-B bonds play key roles in the ultra-incompressibility and hardness of the Nb<sub>2</sub>MB<sub>2</sub>. These findings will inevitably stimulate extensive experimental works on synthesizing these technologically important materials.

## Acknowledgements

This work was financially supported by the National Natural Science Foundation of China Grant Nos.11304140, 11304079 and 11104127 and the Henan Key Teacher Project No. 2014GGJS-114.

## References

- [1] R.B. Kaner, J.J. Gilman, S.H. Tolbert, *Science*. 308(2005)1268.
- [2] J.J. Gilman, R.W. Cumberland, R.B. Kaner, *Int. J. Refract. Met. Hard. Mater.* 24(2006)1.
- [3] J.B. Levine, S.H. Tolbert, R.B. Kaner, *Adv. Funct. Mater.* 19 (2009) 3519.
- [4] V. Brazhkin, N. Dubrovinskaia, M. Nicol, N. Novikov, R. Riedel, V. Solozhenko, Y. Zhao, *Nat. Mater.* 3(2004)576–577.
- [5] R. Wentorf Jr, *J. Chem. Phys.* 26 (1957) 956.
- [6] D.M. Teter, R.J. Hemley, *Science*. 271(1996) 53.
- [7] H.Y. Chung, M.B. Weinberger, J.B. Levine, A. Kavner, J.M. Yang, S.H. Tolbert, R. B. Kaner, *Science*. 316 (2007)436.
- [8] A.M. Locci, R. Licheri, R. Orrù, G. Cao, *Ceram. Int.* 35 (2009)397.
- [9] W. Zhou, H. Wu, T. Yildirim, *Phys. Rev. B.* 76 (2007)184113.
- [10] A.L. Ivanovskii, *Mater. Sci.* 57 (2012) 184.
- [11] W. Zhou, H. Wu, T. Yildirim, *Phys. Rev. B* 76 (2007)184113.
- [12] W. J. Zhao, Y. X. Wang, *J. Solid State Chem.* 182 (2009) 2880.
- [13] A. L. Ivanovskii, *Prog. Mater. Sci.* 57 (2012)184.
- [14] E. Deligoz, K. Colakoglu, Y. O. Ciftci, *Chin. Phys. B*, 21(2012) 106301.
- [15] Y. Pan, W. T. Zheng, W. M. Guan, K. H. Zhang, X. F. Fan, *J. Solid State Chem.* 207 (2013) 29.
- [16] A.G. VanDerGeest, A.N. Kolmogorov, *Calphad.* 46(2014)184.
- [17] K. Takagi, *J. Solid State Chem.* 179 (2006) 2809.

- [18] M. Lukachuk, R. Pöttgen, Z. Kristallogr. 218 (2003) 767.
- [19] B. Y. Kuz'ma, Sov. Powder, Metall. Met. Ceram.10 (1971) 298.
- [20] M. Mbarki, R. S. Touzani, B.P. T. Fokwa, J. Solid State Chem. 203 (2013) 304.
- [21] C.G. Wilson, F.J. Spooner, Acta. Crystallogr. 13 (1960) 358.
- [22] B. Wang, Y. Liu, J. Ye, J. Wang, Comp. Mat. Sci. 70 (2013) 133.
- [23] R.S. Touzani, B.P.T. Fokwa, J. Solid. State. Chem. 211 (2014) 227.
- [24] R.S. Touzani, C.W.G. Rehorn, B. P.T. Fokwa, Comp. Mater. Sci. 104 (2015) 52.
- [25] X.F. Li, Y.P. Tao, Z. Y. Hu, S.L. Zhang, Current. App. Phys..15 (2015) 970.
- [26] G. Kresse, J. Joubert, Phys. Rev. B.59 (1999) 1758.
- [27] H. J. Monkhorst, J. D. Pack, Phys. Rev. B.13 (1976) 5188.
- [28] R. Hill, Proc. Phys. Soc. A 65 (1952) 349.
- [29] T.A. Oba. F, I. Tanaka, Phys. Rev. B.78 (2008)134106.
- [30] F. Birch, Phys. Rev.71 (1947)809.
- [31] F. Mouhat, F.X. Coudert, Phys. Rev. B.90 (2014) 224104.
- [32] S.F. Pugh, Philos. Mag. 45 (1954) 833.
- [33] Wu. Z.J, Zhao. E.J, Xiang. H.P, Hao. X.F, Liu ,X.J, Meng. J, Phys. Rev. B 76 (2007) 054115.
- [34] Chen .X. Q, Niu. H. Y, Li.D. Z, Li .Y. Y, Intermetallics, 19 (2011)1275
- [35] Tian Yongjun, Xu Bo, Zhao Zhisheng, Inte.J. Refract. Metal. Hard Mater/, 33 (2012) 93.
- [36] Y. He, R.B. Schwarz, A. Migliori, J. Mater. Res. 10 (1995) 1187.



The highlights are showed as follows:

- (1) The new compounds  $\text{Nb}_2\text{TcB}_2$  and  $\text{Nb}_2\text{RuB}_2$  are predicted to be synthesized under ambient condition.
- (2) The compounds  $\text{Nb}_2\text{TcB}_2$ ,  $\text{Nb}_2\text{RuB}_2$  and  $\text{Nb}_2\text{OsB}_2$  are mechanically and dynamically stable under high pressure.
- (3) Three compounds are considered to have high elastic anisotropies and superior mechanical properties.